Alzheimer's
Research & Therapy

RESEARCH

Open Access

Plasma lipidomic signatures of dementia with Lewy bodies revealed by machine learning, and compared to alzheimer's disease

Huixin Shen[1†], Yueyi Yu[2†], Jing Wang[5], Yuting Nie[1], Yi Tang[3*] and Miao Qu[1,4*]

Abstract

Background Dementia with Lewy Bodies (DLB) is a complex neurodegenerative disorder that often overlaps clinically with Alzheimer's disease (AD), presenting challenges in accurate diagnosis and underscoring the need for novel biomarkers. Lipidomic emerges as a promising avenue for uncovering disease-specific metabolic alterations and potential biomarkers, particularly as the lipidomics landscape of DLB has not been previously explored. We aim to identify potential diagnostic biomarkers and elucidate the disease's pathophysiological mechanisms.

Methods This study conducted a lipidomic analysis of plasma samples from patients with DLB, AD, and healthy controls (HCs) at Xuanwu Hospital. Untargeted plasma lipidomic profiling was conducted via liquid chromatography coupled with mass spectrometry. Machine learning methods were employed to discern lipidomic signatures specific to DLB and to differentiate it from AD.

Results The study enrolled 159 participants, including 57 with AD, 48 with DLB, and 54 HCs. Significant differences in lipid profiles were observed between the DLB and HC groups, particularly in the classes of sphingolipids and phospholipids. A total of 55 differentially expressed lipid species were identified between DLB and HCs, and 17 between DLB and AD. Correlations were observed linking these lipidomic profiles to clinical parameters like Unified Parkinson's Disease Rating Scale III (UPDRS III) and cognitive scores. Machine learning models demonstrated to be highly effective in distinguishing DLB from both HCs and AD, achieving substantial accuracy through the utilization of specific lipidomic signatures. These include PC(15:0_18:2), PC(15:0_20:5), and SPH(d16:0) for differentiation between DLB and HCs; and a panel includes 13 lipid molecules: four PCs, two PEs, three SPHs, two Cers, and two Hex1Cers for distinguishing DLB from AD.

Conclusions This study presents a novel and comprehensive lipidomic profile of DLB, distinguishing it from AD and HCs. Predominantly, sphingolipids (e.g., ceramides and SPHs) and phospholipids (e.g., PE and PC) were the most dysregulated lipids in relation to DLB patients. The lipidomics panels identified through machine learning may serve as effective plasma biomarkers for diagnosing DLB and differentiating it from AD dementia.

Keywords Dementia with Lewy bodies, Alzheimer's disease, Lipidomic, Biomarker, Machine Learning, Diagnosis

†Huixin Shen and Yueyi Yu contributed equally to the manuscript.

*Correspondence:
Yi Tang
tangyi@xwhosp.org
Miao Qu
qumiao@xwhosp.org
Full list of author information is available at the end of the article

Background

Approximately 55.2 million individuals worldwide are afflicted with dementia, with projections indicating that this number will rise to 139 million by 2050 [1]. Dementia with Lewy Bodies (DLB) accounts for approximately 20% of all dementia cases, second only to Alzheimer's disease (AD) [2]. Clinically, DLB symptoms include cognitive fluctuations with impaired attention and alertness, spontaneous parkinsonism, visual hallucinations, visuospatial dysfunctions, rapid eye movement (REM) sleep behavior disorder (RBD), and marked sensitivity to antipsychotic medications [3, 4]. From a pathological perspective, the development and progression of DLB have been associated with the accumulation and aggregation of α-synuclein in Lewy bodies within the brainstem, limbic system, and neocortical regions [4, 5].

DLB was recognized as a distinct entity only two decades ago, owing to its clinical heterogeneity and overlap with other neurodegenerative conditions. The diagnostic criteria for DLB have undergone changes over time, with revisions occurring in 2005 and again in 2017 [3, 6]. The diagnostic criteria for DLB also incorporate indicative techniques such as positron emission computed tomography (PET), single-photon emission computed tomography (SPECT), and polysomnography (PSG), along with supportive techniques including magnetic resonance imaging (MRI) and electroencephalography (EEG) [3]. However, these techniques may lack specificity or involve the use of radioactive substances. Furthermore, due to the clinical and neuropsychological similarities between DLB and AD, arriving at a definitive diagnosis for DLB can be challenging. Indeed, many of the clinical symptoms of DLB closely resemble those of AD, particularly in the early stages of the pathology, with deficits in episodic memory, short-term memory, and working memory being particularly common [7].

Thus, the dearth of early diagnosis underscores the significance of identifying non-invasive biomarkers. Accordingly, it is imperative to explore novel biomarkers that can effectively differentiate DLB from AD and thus improve differential diagnosis. Blood metabolites have recently emerged as a promising avenue for identifying biomarkers in neurodegenerative disorders, particularly in the case of AD [8–11]. Lipidomics, a branch of metabolomics, systematically identifies and profiles lipids across various classes and species in biological samples. This approach, contrasting to traditional methods, offers enhanced potential for uncovering mechanisms in slowly progressing diseases by integrating lipid profiles with biological phenotypes based on its ability to accurately reflect the ongoing changes in chronic conditions [12, 13], making it a valuable tool in the search for disease-associated biomarkers.

Several previous blood metabolomic studies have emphasized the role of lipid compounds in AD [9, 14, 15], as well as investigating the interaction between α-synuclein and lipids [16, 17]. However, no systematic studies have been conducted to examine the plasma lipid metabolism in individuals with DLB.

In addition, machine learning could efficiently process extensive metabolomics data, automatically select the most pertinent metabolite profiles, and diminish the requirement for human intervention, consequently augmenting the intricacy, stability, and explicability of predictive models. Thus, machine-learning approaches have recently been applied to the diagnostic prediction of AD with several separate analytes, including those measured by cerebrospinal fluid biomarkers [18] and plasma biomarkers [19]. However, the application of machine learning for diagnosing and differentiating DLB has not yet been reported.

In this study, we conducted lipidomics analyses on DLB patients, compared with AD and healthy controls (HCs). Our objective was to discover novel lipids and lipid panel associated with clinical DLB diagnosis and DLB endophenotypes, such as cognitive function and parkinsonism features, and to identify differences in lipid metabolism between individuals with AD and DLB using machine learning. Our study is pioneering in utilizing plasma lipidomic markers to generate a model capable of predicting and discriminating DLB patients from HCs and AD patients. To our knowledge, this is the first one and most comprehensive blood lipidomic analysis in DLB to date, aimed at identifying lipid signatures associated with DLB and DLB endophenotypes. We anticipate that our findings will significantly enhance understanding of the molecular mechanisms associated with DLB, aiding in early diagnosis and the identification of new therapeutic targets.

Materials

Study participants

This research was conducted in the memory ward at Xuanwu Hospital, Capital Medical University, Beijing, China, from August 2021 to June 2022. The study population comprised patients diagnosed with DLB and AD, selected from the memory ward. Additionally, a HC group was enrolled from the local community through advertising. The study design adhered to the principles outlined in the Declaration of Helsinki. The Ethics Committee of Xuanwu Hospital, Capital Medical University, granted approval for our study (approval No. [2020]141), and informed consent was obtained from all participants.

AD diagnosis [20] was based on the National Institute of Aging and the Alzheimer's Association (NIA-AA). Patients with AD underwent lumbar puncture and

^{11}C-Pittsburgh Compound B-positron emission tomography (^{11}C-PiB-PET) examination, meeting the criteria outlined in the 2018 NIA-AA Research Framework [21], which provided the ATN system (amyloid [A], tau [T], and neurodegeneration [N]) as a biological staging model for AD. DLB diagnosis followed the International Consensus criteria [22]. AD and DLB diagnoses were established by a consensus panel consisting of three experienced neurologists. The HC group were volunteers without cognitive decline, achieving a Montreal Cognitive Assessment (MoCA) score over 26 points, along with a Clinical Dementia Rating Scale (CDR) score of 0. Individuals with the following conditions were excluded: mixed dementia; severe physical, or psychiatric disorder; a history or current excessive alcohol consumption; and the use of psychotropic drugs; as well as those with systemic inflammatory disorders or autoimmune diseases. Additionally, we conducted extensive genetic screening on AD patients to exclude gene variants that could potentially lead to early-onset dementia.

Patients were assessed by an experienced medical practitioner, encompassing both physical and neurological examinations. The evaluation of parkinsonism utilized the Movement Disorder Society Unified Parkinson's Disease Rating Scale (UPDRS), while cognitive function was assessed through the Clock Drawing Test (CDT), Mini-Mental State Examination (MMSE), MoCA, and CDR.

Plasma sample collection for lipidomics

Blood samples were obtained from all participants in this study. We adhered to recommended best practices for the pre-analytical processing of the plasma samples for lipidomics analysis [23]. Approximately 6 mL of venous blood was collected using Ethylenediaminetetraacetic acid (EDTA) tubes (BD, USA) and centrifuged at 1300 g for 10 minutes at 4 °C to separate the plasma. The plasma was then aliquoted into 0.5 mL portions in polypropylene tubes and stored. The plasma samples (200 µL of processed plasma) were preserved at -80 °C for 3–10 months without repeated freeze-thaw cycles. They were subsequently transported in dry ice to the Applied Protein Technology Company (Shanghai, China) for lipidomics analysis. Upon arrival, the samples were maintained at -80 °C for two weeks before being thawed for the untargeted lipidomics analysis.

Untargeted lipidomic profiling of plasma samples

Lipid extraction and mass spectrometry (MS)-based lipid detection were conducted as previously [24, 25] and facilitated by the Applied Protein Technology Co., Ltd., Shanghai, China. The lipidomic profile of the plasma from the patients was assessed using untargeted lipidomic analysis. The lipid extraction method was as follows: The lipid extraction method involved placing the sample in a 1.5 mL tube, adding 200 µL water, and vortexing at 4 °C. 240 µL of pre-cold methyl alcohol was added, followed by vortexing, and 800 µL of MTBE was added and the mixture was sonicated at 4 °C for 20 min followed by sitting still for 30 min at room temperature. The solution was centrifuged at 14,000 g for 15 min at 10°C and the upper organic solvent layer was obtained and dried under nitrogen. The lipid extracts were analyzed via ultra-high-performance liquid chromatography (UHPLC) coupled with electrospray ionization quadrupole time-of-flight (ESI-Q-TOF) tandem mass spectrometry (MS/MS). UHPLC employed a CSH C18 column, and mass spectral analysis was performed using a Q-Exactive Plus in both ion modes.

Lipid identification

LipidSearch 4.1 in our study (ThermoFisher Scientific, Waltham, MA, USA) [26, 27] was used for identifying lipid species, including peak extraction, peak alignment, and quantification. The LipidSearch includes over 30 lipid classes and more than 1,500,000 ion fragments. Mass tolerances were maintained at 5 ppm for both molecular precursors and fragment ions, with a product ion display threshold of five. All lipid classes in this database were chosen for identification.

Data processing and statistical analysis

Descriptive statistics were used to summarize the study population's characteristics. Data normality was assessed using the Shapiro-Wilk test. Continuous variables were presented as mean (standard deviation) for normally distributed data and the median (25th; 75th percentile) for non-normally distributed data. Categorical data were reported as frequency (percentage). Group comparisons were conducted using analysis of variance (ANOVA) or Kruskal-Wallis tests for quantitative data, and chi-squared tests for categorical data, with post-hoc pairwise (Dunn-Bonferroni) corrections. Significance was set at $p < 0.05$. Lipids significantly different between groups ($p < 0.05$, variable importance for the projection (VIP)>1) were identified as differentially expressed. Differences in the expression of lipid species were tested using analysis of covariance (ANCOVA) with adjustment for the age and gender. Correlations between differentially expressed lipids and clinical parameters were analysed by Spearman correlation. Analyses were performed using SPSS Statistics software (IBM, version 25).

Lipidomic data were processed using LipidSearch software, normalized via Pareto scaling, and analyzed using SIMCA-P 14.1 (Umetrics, Umea, Sweden) for multivariate analyses, including principal component analysis, partial least squares discriminant analysis, and

orthogonal partial least squares discriminant analysis (OPLS-DA). Significantly expressed lipids were identified by combining thresholds from OPLS-DA and two-tailed Student's *t*-tests, along with mapping of volcano, hierarchical-cluster, and correlation analyses using R software.

An integrated machine learning methodology was employed to assign values to the chosen biomarkers by amalgamating various feature selection techniques. The cumulative weight for each marker was subsequently computed to discriminate between samples from the DLB and AD/HC groups. Then, the receiver-operating characteristic (ROC) analysis evaluated the impact of biomarkers on the model's Area Under the Curve (AUC) value, with high AUC values indicating better classification results. Finally, machine learning models, including logistic regression, random forest, and support vector machine, were employed to validate the screening outcomes, and the ROC curve analysis was used to assess the performance of biomarkers in classifying distinct sample groups. R version 4.0.2 was used for all statistical analyses.

Results

Characteristics of samples

This study incorporated and analysed 159 consecutive cases, each accompanied by clinical data and plasma samples. Of these individuals, 57 had AD, 48 had DLB, and 54 were cognitively unimpaired HCs. The median age of the DLB group was significantly older compared to both the AD ($p<0.001$) and HC groups ($p=0.005$). Furthermore, the DLB cohort had a higher proportion of male participants compared with the HC ($p=0.006$) and AD groups ($p=0.009$). However, there were no significant differences in education level, body mass index (BMI), prevalence of hypertension, diabetes, hyperlipidemia, and stroke across the groups. The AD and DLB groups demonstrated impairments in various neuropsychological tests including the MMSE, MoCA, CDT, and CDR compared to HCs. There were no significant differences in MMSE, MoCA, CDT, and CDR total scores between the DLB and AD groups. Regarding specific clinical features of DLB, the average UPDRS score was 68 (IQR 40–109) points. Patients with DLB demonstrated a range of symptoms including parkinsonism (96%), visual hallucinations (83.3%), RBD (64.6%), and cognitive fluctuations (41.7%). Table 1 presents the detailed demographic and clinical profiles of all participants.

Results are presented as median with Lower Quartile (LQ) to Upper Quartile (UQ) below. Statistical tests are denoted with symbols. †Significantly different from control group ($p\leq0.05$); ‡Significantly different from AD group ($p\leq0.05$). Abbreviation: HC, healthy control; AD, Alzheimer's diseases; DLB, dementia with Lewy bodies; BMI, body mass index; HDL, high-density lipoprotein;

Table 1 Participant demographics and clinical characteristics

Variables	HC ($n=54$)	AD ($n=57$)	DLB ($n=48$)	*P* value
Age [years, M (Q_1, Q_3)]	67.5 (63, 71)	63 (57, 72)	71 (67, 78) †‡	< 0.001
Gender, males/females	20/34	23/34	30/18 †‡	0.015
Education [years, M (Q_1, Q_3)]	12 (9, 15)	10 (9, 14)	12 (9, 16)	0.224
BMI (kg/m^2)	24.75 ± 2.98	23.48 ± 3.23	29.90 ± 3.27	0.087
Hypertension, *n* (%)	23 (42.6%)	18 (32.1%)	24 (50.0%)	0.176
Diabetes, *n* (%)	7 (13.0%)	5 (8.9%)	11 (22.9%)	0.120
Stroke, *n* (%)	4 (7.4%)	4 (7.1%)	5 (10.4%)	0.803
Aspirin intake, *n* (%)	10 (18.5%)	7 (12.5%)	8 (16.7%)	0.676
LDL (mmol/L)	2.91 ± 0.99	2.76 ± 0.85	2.49 ± 0.89	0.077
HDL (mmol/L)	1.43 ± 0.34	1.38 ± 0.33	1.32 ± 0.42	0.260
TC (mmol/L)	4.98 ± 0.94	4.70 ± 0.95	4.59 ± 0.91	0.098
TG (mmol/L)	1.71 ± 0.97	1.40 ± 0.84	1.29 ± 1.08	0.088
MMSE [scores, M (Q_1, Q_3)]	28 (28, 29)	18 (13, 22) †	21 (14, 24) †	< 0.001
MoCA [scores, M (Q_1, Q_3)]	26 (24, 27)	13 (8, 17) †	13 (8, 19) †	< 0.001
CDT [scores, M (Q_1, Q_3)]	3 (3, 3)	1 (0, 2) †	1 (1, 2) †	< 0.001
CDR [scores, M (Q_1, Q_3)]	0 (0, 0)	1 (1, 2) †	1 (1, 2) †	< 0.001
UPDRS [scores, M (Q_1, Q_3)]	N/A	/	68 (40, 109)	/
Visual hallucinations, *n* (%)	N/A	/	40 (83.3%)	/
Fluctuations, *n* (%)	N/A	/	20 (41.7%)	/
Parkinsonism, *n* (%)	N/A	/	48 (96%)	/
RBD, *n* (%)	N/A	/	31 (64.6%)	/

LDL, low-density lipoprotein; TC, total cholesterol; TG, triglyceride; MMSE, Mini-Mental State Examination; MoCA, Montreal cognitive assessment; CDT, Clock Drawing Test; CDR, Clinical Dementia Rating Scale; UPDRS, Unified Parkinson's Disease Rating Scale; RBD, REM sleep behavior disorder.

Different lipidomic profiling between the DLB and HC Groups and correlation with clinical parameters

The first objective of this study was to assess the differences in lipid groups between DLB patients and HCs to characterize plasma lipidomic profiling in DLB patients. Non-targeted lipidomics was conducted using liquid chromatography coupled to MS (LC/MS). After quality control, a total of 33 lipid classes and 1527 lipid species were identified in the analyses. Principal component analysis (PCA) of the lipidome data from both the samples and quality controls QCs confirmed the high quality of the data.

Significant differences were observed between the HC and DLB groups in several lipid classes. The levels of sphingosine (SPH) (p<0.001), trihexosyl N-acetylhexosyl ceramide (CerG3GNAc1) (p <0.001), hexosylceramide (Hex1Cer) (p=0.007), trihexosylceramide (Hex3Cer) (p = 0.002), wax esters (WE) (p<0.001), and lysophosphatidylglycerol (LPG) (p<0.001) were significantly higher in the DLB group. In contrast, the levels of cardiolipin (CL) (p=0.045), fatty acids (FA) (p=0.038) and phosphatidic acid (PA) (p<0.001) were markedly reduced in the DLB group (Fig. 1). ROC analysis was conducted to confirm the diagnostic accuracy of this lipid classes in distinguishing patients with DLB from HCs. As shown in Fig. 2A, the AUC for SPH was >0.9, indicating high diagnostic reliability. This suggests that changes in SPH levels might be potential biomarkers for DLB diagnosis at the class level, potentially elucidating pathways in sphingolipid metabolism. The AUC was 0.950 for a lipid class signature predicting DLB, which composed of 6 lipid classes (SPH, WE, LPG, CerG3GNAc1, Hex1Cer and Hex3Cer) (Fig. 2B).

Lipidomic analysis additionally demonstrated distinct variations in lipid at the species levels between the DLB and HC groups. Using the OPLS-DA model, sixty-eight lipid species were identified that distinguished DLB patients from HCs (Supplementary Table S1). After adjusting for confounders such as age and gender, a total of 55 differentially expressed lipid species were confirmed, with 31 species lower and 24 species higher in the DLB group compared to HCs (Fig. 3, Supplementary Table S2).

Correlation analyses showed that SM(d42:0)+HCOO (R = -0.469, p=0.049) and SPH(d16:0)+H (R = -0.606, p=0.007) negatively correlated with UPDRS III scores, indicating a relationship between these lipids and the severity of movement symptoms in DLB. Additionally, levels of various ceramides (Cers) (e.g., Cer(d18:1_16:0)+HCOO) and sphingolipids (e.g., SM(d42:1)+HCOO) negatively correlated with MMSE, MoCA, and CDT scores, yet positively correlating with CDR scores, suggesting a link between lipid changes and cognitive symptoms severity in DLB (Fig. 4).

Different lipidomic profiling between the DLB and AD groups and correlation with clinical parameters

Then, we assessed the differences in lipid profiles between patients with DLB and AD to distinguish these two dementia types and investigate their underlying mechanisms. The levels of dihexosyl N-acetylhexosyl ceramide (CerG2GNAc1) (p<0.001), CerG3GNAc1 (p<0.001), FA (p=0.005), lysophosphatidylethanolamine (LPE) (p=0.024), lysophosphatidylinositol (LPI) (p<0.001), Hex1Cer (p=0.037), Hex3Cer (p=0.037),

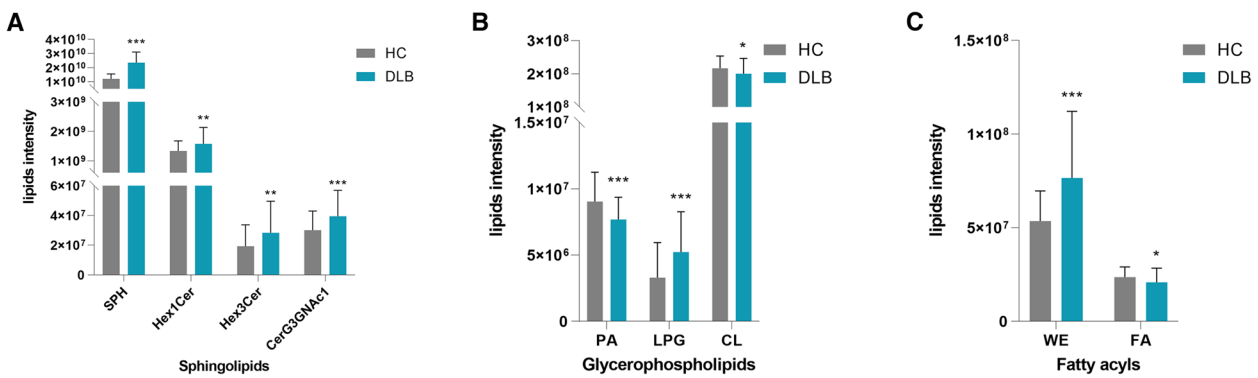

Fig. 1 Different lipid class between the DLB and HC groups. Abbreviation: DLB, dementia with Lewy bodies; HC, Healthy controls; SPH, sphingosine; Hex1Cer, hexosylceramide; Hex3Cer, trihexosylceramide; CerG3GNAc1, trihexosyl N-acetylhexosyl ceramide; PA, phosphatidic acid; LPG, lysophosphatidylglycerol; CL, cardiolipin; WE, wax esters; FA, fatty acids. *p < 0.05 vs. HC;** p < 0.01 vs. HC; *** p < 0.001 vs. HC

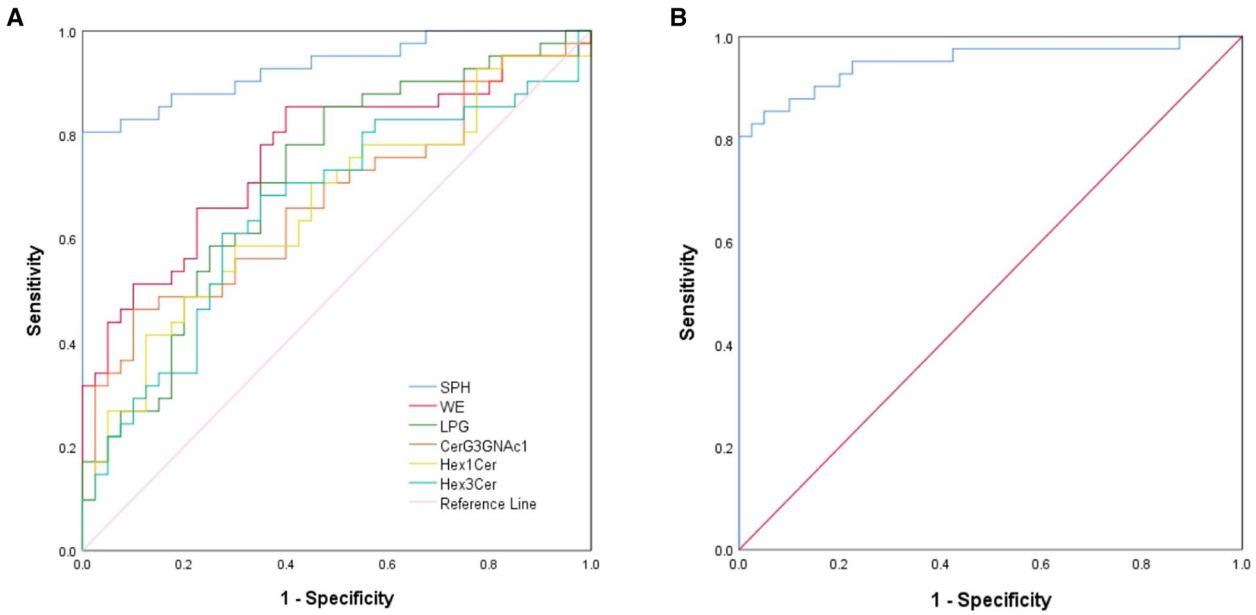

Fig. 2 **A** Receiver operating characteristic (ROC) curve of various lipid classes used to differentiate between DLB and HC.**B** ROC curves of the six lipid classes for joint prediction of DLB. Abbreviation: DLB, dementia with Lewy bodies; HC, Healthy controls; SPH: sphingosine; WE, wax esters; LPG, lysophosphatidylglycerol; CerG3GNAc1, trihexosyl N-acetylhexosyl ceramide; Hex1Cer, hexosylceramide; Hex3Cer, trihexosylceramide

and ChE (cholesteryl ester) ($p=0.040$) were significantly higher in DLB group, whereas the levels of SPH ($p=0.047$) and LPG ($p<0.001$) were significantly lower in DLB group (Fig. 5). ROC analysis indicated that LPG and LPI had AUCs of 0.757 and 0.720, respectively, indicating high reliability (Figs. 6A). The ROC was 0.874 for a lipid class signature in predicting DLB, composed of nine lipid classes (LPG, LPI, CerG2GNAc1, CerG3GNAc1, Hex1Cer, Hex3Cer, FA, SPH and LPE) (Figs. 6B).

In total, 23 lipid species were identified that distinguished DLB patients from AD (Supplementary Table S3). After adjusting for confounding factors (age and sex), lipidomic profiling 17 differentially expressed lipid species in DLB compared to AD patients, with 7 species exhibiting lower levels and 10 at higher levels. Significant changes in lipid levels between the DLB and AD groups are detailed in Supplementary Table S4 and Fig. 7. Further analysis revealed a correlation between specific lipid species and clinical parameters. Hex1Cer(d18:1_23:0)+HCOO was negatively correlated with the MMSE scores (R = -0.30, $p=0.042$) in DLB group. Conversely, the level of PE(18:0p_20:4)+H showed a positive correlation with UPDRS III scores ($R=0.47$, $p=0.046$).

Lipidomic predication model for DLB

The subsequent objective of this investigation was to identify plasma lipidomic signatures that could facilitate the identification of individuals with DLB. A predictive model was constructed using machine learning methods. Multivariate analysis of variable selection showed that the specific fingerprint distinguishing DLB from HC comprised three lipid species (Fig. 8A): PC(15:0_18:2)+HCOO, PC(15:0_20:5)+HCOO, SPH(d16:0)+H. Conversely, the lipidomic signature differentiating DLB from AD consisted of 13 lipid species, including four PCs, two PEs, three SPHs, two Cers, and two Hex1Cers. These specific lipid species are as follows: Cer(t18:0_22:0)+HCOO, Cer(d18:1_24:2)+HCOO, SPH(d16:0)+H, SPH(d18:0)+H, SPH(d22:0)+H, PE(20:1e_20:3)-H, PE(18:2e_20:4)-H, PC(32:0e)+H, PC(44:6e)+H, PC(15:0_20:5)+HCOO, PC(15:0_18:2)+HCOO, Hex1Cer(d18:1_24:0)+HCOO, and Hex1Cer(d18:1_23:0)+HCOO. The predictive efficacy of these lipidomic fingerprints was demonstrated by an AUC of 1 for distinguishing DLB from HC, and an AUC of 0.77 for differentiating DLB from AD (Fig. 8B).

Discussion

To our best knowledge, our study presents the first comprehensive lipidomic profile analysis in DLB patients, comparing it not only to HCs but also to AD. Our results suggest potential diagnostic value of these lipidomic profiles as biomarkers, and it also highlights several key biological processes that may be relevant to the pathogenesis of DLB. Firstly, we identified 55 plasma lipids exhibiting differential levels between DLB patients and HCs, alongside 17 plasma lipids that varied between DLB patients and AD patients, even when accounting for confounding

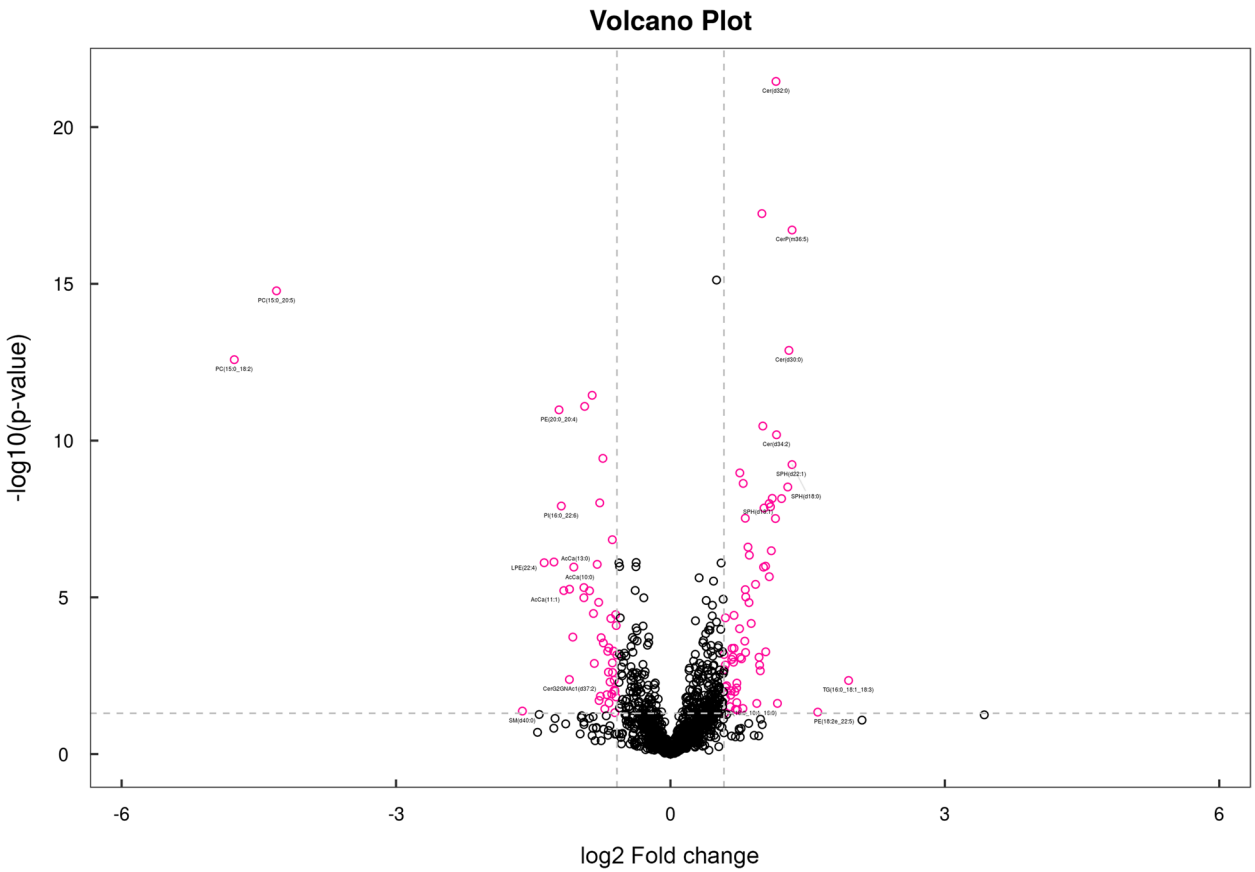

Fig. 3 Volcano plots of the Fold change (FC) (x-axis) and *p*-value (y-axis) for each detected lipid in the comparison of DLB vs. HC subjects. Red dots represent significantly upregulated (FC> 1.5) molecules or downregulated (FC <0.67) molecules in DLB patients. Abbreviation: DLB, dementia with Lewy bodies; HC, Healthy controls

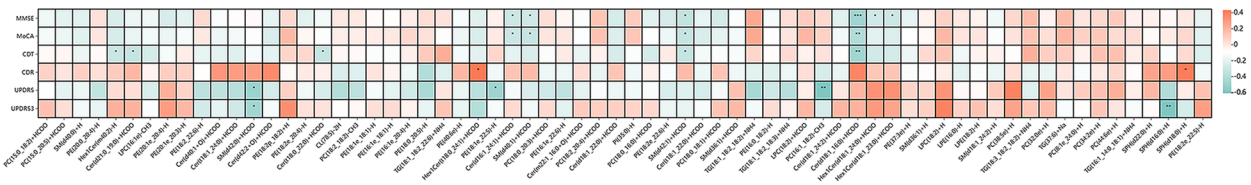

Fig. 4 Significant correlations between clinical parameters of DLB patients and the differentially expressed lipids species. The colour scale illustrates the degree of correlation and ranges from red to green, indicating negative and positive correlations, respectively. Abbreviation: DLB, dementia with Lewy bodies; MMSE, Mini-Mental State Examination; MoCA, Montreal Cognitive Assessment; CDT, Clock Drawing Test; CDR, Clinical Dementia Rating Scale; UPDRS, Movement Disorder Society Unified Parkinson's Disease Rating Scale

factors. Notably, the lipids that showed differential expression were primarily sphingolipids and phospholipids, both at the class and species levels. Secondly, through machine learning multivariate analyses, we identified a lipid panel that demonstrated high accuracy in differentiating DLB patients from HCs, and another lipid panel efficacious in distinguishing DLB from AD. Thirdly, significant correlations were observed between these lipidomic profiles and both UPDRS III and cognitive scores, indicating their relevance to the severity of DLB symptoms.

Change of sphingolipids metabolism

In our study focusing on sphingolipids, SPHs in plasma were significantly higher in DLB subjects relative to HCs, while lower than in those with AD patients. Furthermore, a range of Cers, including Hex1Cer, Hex3Cer, CerG3GNAc1, and CerG2GNAc1, demonstrated elevated

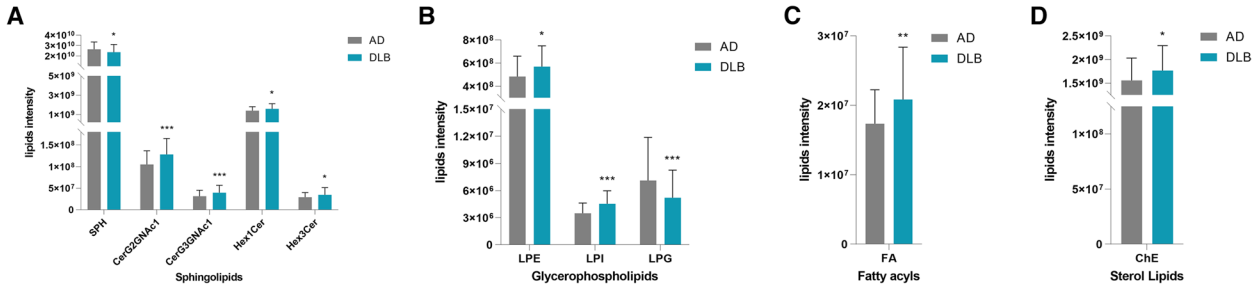

Fig. 5 Different lipid class between the DLB and AD groups. Abbreviation: DLB, dementia with Lewy bodies; AD, Alzheimer's disease; SPH, sphingosine; CerG2GNAc1, dihexosyl N-acetylhexosyl ceramide; CerG3GNAc1, trihexosyl N-acetylhexosyl ceramide; Hex1Cer, hexosylceramide; Hex3Cer, trihexosylceramide; LPE, lysophosphatidylethanolamine; LPI, lysophosphatidylinositol; LPG, lysophosphatidylglycerol; FA, fatty acids, ChE, cholesteryl ester. *$p < 0.05$ vs. AD; ** $p < 0.01$ vs. AD; *** $p < 0.001$ vs. AD

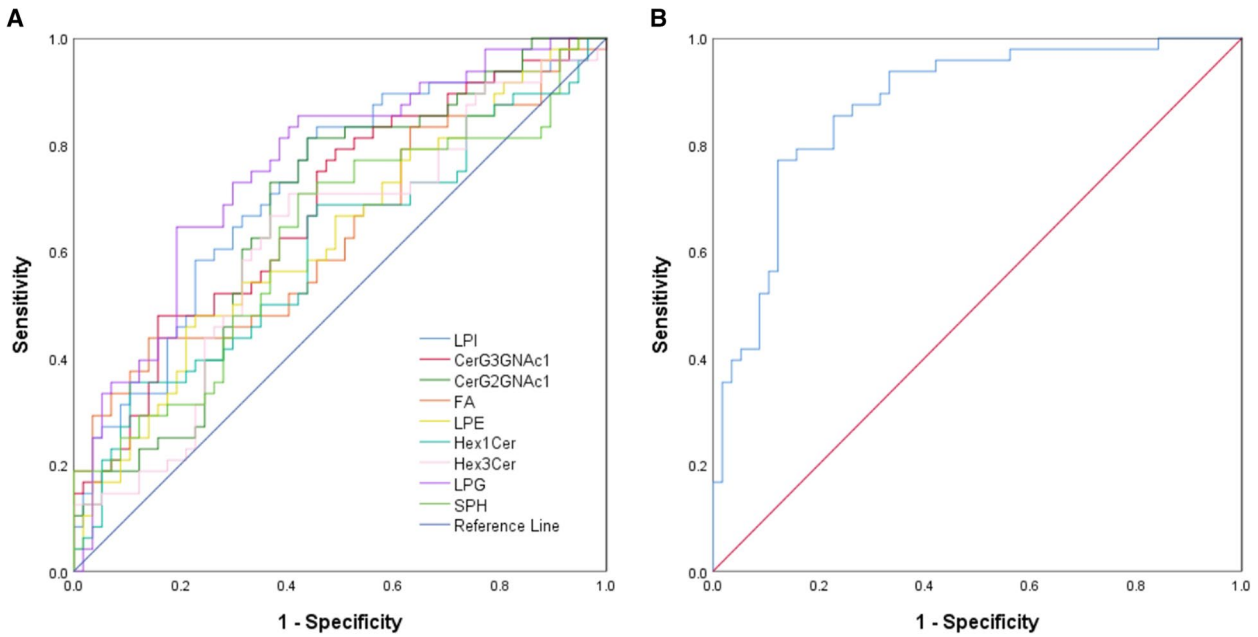

Fig. 6 **A** Receiver operating characteristic (ROC) curve of various lipid classes used to differentiate between DLB and AD. **B** ROC curves of the nine lipid classes for joint prediction of DLB. DLB, dementia with Lewy bodies; AD, Alzheimer's disease; SPH, sphingosine; CerG2GNAc1, dihexosyl N-acetylhexosyl ceramide; CerG3GNAc1, trihexosyl N-acetylhexosyl ceramide; Hex1Cer, hexosylceramide; Hex3Cer, trihexosylceramide; LPE, lysophosphatidylethanolamine; LPI, lysophosphatidylinositol; LPG, lysophosphatidylglycerol; FA, fatty acids

plasma levels in DLB patients relative to both AD subjects and HCs. In addition, machine learning models indicated alterations in sphingolipid metabolism, including the upregulation of SPH(d16:0) + H in the model differentiating DLB from HCs, and the downregulation of Hex1Cer(d41:1) + HCOO in the model distinguishing DLB from AD.

Sphingolipids, a lipid category with a sphingoid base as their backbone, are modified to form Cers, SM, and glycosphingolipids. There are several hundred different types of sphingolipids, many of which are integral to a variety of physiological processes. Notably, certain sphingolipids such as Cers, SPH, Sph-1-phosphate (S1P), and Cer-1-phosphate (C1P) serve as bioactive molecules and play crucial roles in various cellular activities including signal transduction modulation, protein sorting, and facilitating cell-to-cell interactions and recognition mechanisms [28]. Thus, any perturbation in sphingolipid metabolism can alter plasma membrane organization and has been linked to the pathogenesis of a range of neurodegenerative disorders such as AD, various cancers, and the metabolic syndrome [29, 30].

Our findings are consistent with previous research regarding patients with cognitive impairments. Several

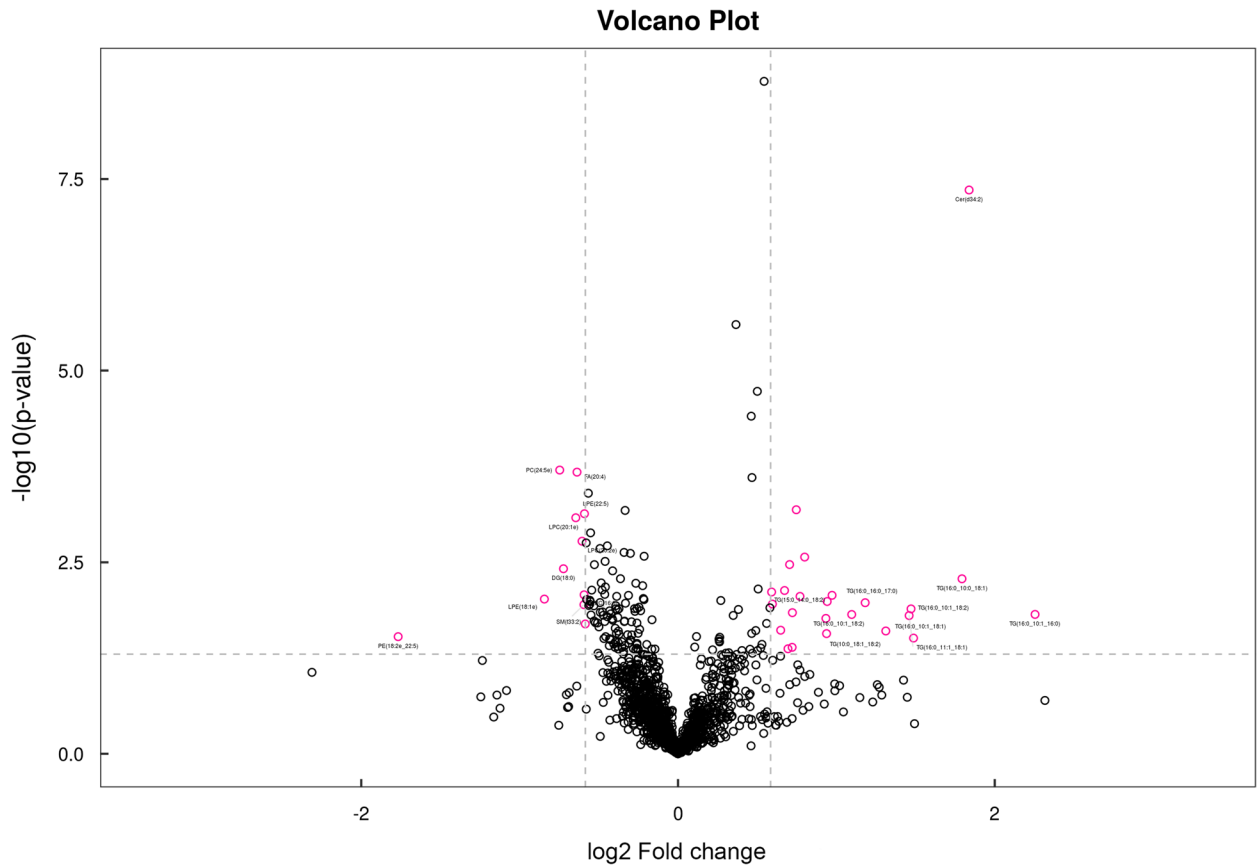

Fig. 7 Volcano plots of the Fold change (FC) (x-axis) and *p*-value (y-axis) for each detected lipid in the comparison of DLB vs. AD subjects. Red dots represent significantly upregulated (FC> 1.5) molecules or downregulated (FC <0.67) molecules in DLB patients. DLB: dementia with Lewy bodies, AD: Alzheimer's disease

studies have shown elevated levels of SPH in the brain tissues of AD patients compared to HCs [31–33]. Furthermore, a plasma-based study found significantly higher SPH levels in patients with cognitive impairments [34]. Additionally, in the Women's Health and Aging Study (WHAS) II, a longitudinal study involving 100 women with up to six follow-ups over nine years, higher serum Cers levels could predict memory impairment over the follow-up [35]. Cers is synthesized from serine and palmitoyl Coenzyme A, as well as through the acylation of SPH in the endoplasmic reticulum, in the meanwhile SPH is produced via the hydrolysis of Cers [36]. Given that Cer and SPH are interconvertible, their synergistic elevation in plasma levels within the pathological context of DLB in our study is a logical outcome.

Furthermore, research examining the correlations between sphingolipids and clinical evaluations has revealed new discoveries. DLB and Parkinson's disease (PD) share clinical and neuropathological features, both falling under the spectrum of Lewy body diseases (LBDs) [37]. A previous comparative study of PD patients revealed that higher Cer levels and monohexadecylglyceramide were associated with poorer cognitive function [38], but no studies have identified a correlation between motor function and sphingolipid levels. Surprisingly, our study found a negative correlation between certain sphingolipids (lipid classes such as SPH, lipid species such as SM(d42:0) + HCOO and SPH(d16:0) + H) and movement function in DLB patients. This observation suggests a potential relationship between sphingolipid variability and motor symptom severity in DLB. Our results are supported by research focusing on PD patients, which have demonstrated that serum S1P levels, a type of sphingolipid, were inversely correlated with motor impairment severity, as measured by UPDRS III score [39]. S1P agonists have been observed to confer protection to dopaminergic neurons against cell death induced by 1-methyl-4-phenylpyridinium (MPP), and S1P signaling has been found to exert neuroprotective effects in murine models of PD [40, 41]. Importantly, S1P is converted to SPH through the Sphingosine-1-Phosphate Phosphatases (SPPs) [42]. Consequently, the observed correlation

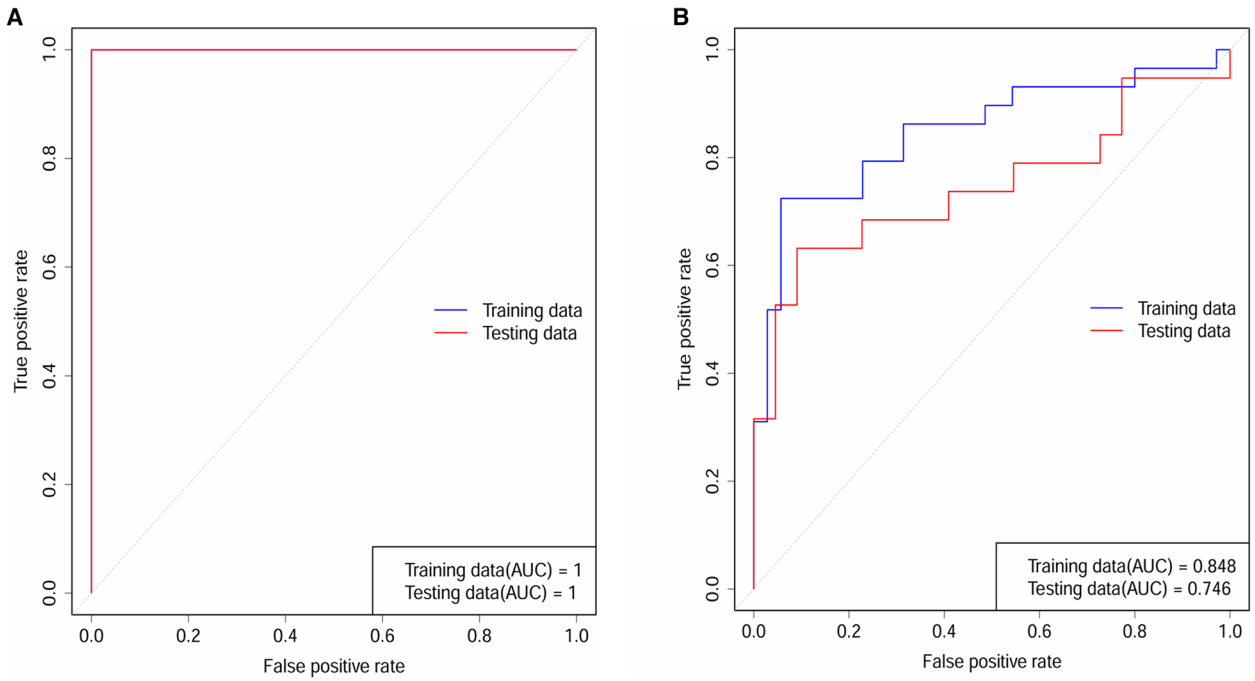

Fig. 8 **A** Model performance in distinguishing DLB from HC, (**B**) Model performance in distinguishing DLB from AD. DLB: dementia with Lewy bodies, HC: Healthy controls, AD: Alzheimer's disease

between SPH levels and UPDRS III scores in our study appears plausible, and could provide avenues for further deeper investigations into motor dysfunction and sphingolipid metabolism in DLB patients in the future.

There are several persuasive mechanisms for delving deeper into the elevation of Cers and SPH, which might help explain our findings of significantly higher SPH levels in AD compared to the DLB group: 1) Research into the sphingolipid metabolic pathway in AD [43] indicated that the majority of altered gene expression within sphingolipid metabolic pathway occurred in temporal and frontal cortices brain regions notably affected early in AD compared to the normal aging process. The study also found an early upregulation of enzymes responsible for synthesizing Cers, especially those with long-chain Cers, during the progression of the disease. 2) Two studies also reported increased activity of acid ceramidase, an enzyme that converts Cer to SPH in AD brains when compared with normal controls [44, 45]. We can infer from the aforementioned studies that in the progression of AD pathology, the upregulation of Cer synthesis enzymes facilitated the conversion of Cer to SPH, resulting in elevated SPH levels.

However, to date, no studies have directly investigated SPH or relevant enzymes in DLB patients to determine their potential disruption in the disease's pathogenesis. It is worth noting that DLB and PD exhibit overlapping pathophysiological mechanisms. Two studies [46, 47] have suggested an association between sphingolipid metabolism and the pathogenesis of PD. In PD patients, there was an increase in the expression of enzymes involved in Cer synthesis within the anterior cingulate cortex, a specific brain region that contains α-synuclein pathology of Braak Stage IV [47]. Concurrently, elevated Cers levels were detected in post-mortem brain tissues of PD patients [46]. A similar pattern of sphingolipid accumulation is observed in α-synuclein aggregation, a marker of DLB. The overexpression of α-synuclein disrupts the Cer/SM recycling pathway, thus promoting the synthesis of Cers [48]. This leads to its accumulation and ultimately resulting in neurodegeneration. All the above studies support our findings, which identified heightened levels of Cers in DLB patients.

However, our model also identified a downregulation in certain Cer metabolites, that might be explained by mutations in the glucocerebrosidase (GCase) gene. An increasing number of literatures report that mutations in the GCase gene increased susceptibility to PD development [49, 50]. GCase, a lysosomal enzyme, is crucial for metabolizing glucosylceramide into free Cers and glucose [29]. Additionally, GCase play a vital role in degrading α-synuclein, protecting against α-synuclein aggregation in the brain. Recently, researches have documented a reduction GCase activity in the brain of PD patients

[51, 52]. The insufficient GCase activity may result in decreased Cers levels, impair the α-synuclein degradation, and consequently leads to its intracellular aggregation [53].

Change of phospholipid metabolism

In addition to sphingolipids, we also observed differences in phospholipid expression profiles among DLB, AD, and HC. Notably, our research found that plasma PA levels were significantly lower in DLB compared to HCs. Using machine learning models, we identified a downregulation of PC(16:1_18:2) + HCOO in the DLB group, while PC(44:6e) + H was downregulated in AD. These findings are supported by several studies conducted on brain tissue and plasma from individuals with α-synucleinopathies.

PC and PE, which are the predominant glycerophospholipids in cell membranes, are synthesized from PA through the Kennedy pathway [54], so it is reasonable to deduce that alterations in the levels of these three components imply a strong correlation in DLB patients. Previous studies have consistently revealed a decrease in PE and PC levels in the brain tissues of PD patients [55, 56]. Notably, a decline in PC species with polyunsaturated fatty acyl side chains (denoted as 34:5, 36:5, and 38:5), has been observed in the frontal cortex of PD brains [56]. Some studies involving the plasma of PD patients have reported the decrease in levels of PC 35:6 and PE 34:1 [57, 58].

These changes in polyunsaturated fatty acid might result from α-synuclein accumulation on cell membranes of neuron, as trends of lower PC species have been observed in yeast and rat models of cortical neuron with excess α-synuclein [30]. Additionally, α-synuclein has an affinity for negatively charged phospholipids such as PE, PA, and phosphatidylglycerol (PG). Lipid environments containing these negatively charged phospholipids have been shown to trigger, accelerate or inhibit α-synuclein aggregation [59–62]. Specifically, PA esterified with saturated or monounsaturated fatty acids are favored for α-synuclein attachment, potentially enhancing protein aggregation by inducing alterations in the protein's secondary structure [63]. In vitro studies show that removing phosphatidylserine decarboxylase (PSD1), responsible for converting PS into PE, increased cytoplasmic α-synuclein inclusion formation and enhanced α-synuclein toxicity in a yeast model. Significantly, in a Caenorhabditis elegans model of α-synucleinopathy, silencing PSD1 RNAi exacerbated dopaminergic neuron degeneration caused by wild-type human α-synuclein [47]. The above studies collectively indicate a strong association between α-synuclein and PE and PC metabolites. Nevertheless, the causal connection between alterations in PC and PE levels in individuals with DLB and α-synuclein aggregation remains uncertain. To establish and confirm this relationship, further longitudinal investigation is crucial.

In summary, our results indicate that alterations in both sphingolipid and phospholipids metabolism might play an important role in the pathobiology of DLB. In multivariate analyses using machine learning, the evaluation of plasma levels of these lipid species could facilitate the diagnosis of DLB and its differentiation from AD through a non-invasive, simple to perform, and cost-effective testing approach.

Our study has several strengths. Primarily, it represents the first lipidomic examination of the DLB group, comparing DLB patients not only with HC but also with AD cohorts to identify metabolic signatures distinguishing between these two neurodegenerative disorders. Furthermore, the study sample was sourced from the Cognitive Neurology Ward at Xuanwu Hospital, Capital Medical University, which is a national clinical center for neurodegenerative diseases and memory disorders in China, thereby ensuring meticulous diagnostic processes and the reliability and completeness of data. Additionally, we applied a machine learning model to optimize the selection of lipid molecule combinations for diagnosis and identification. It is important to recognize the significance of pre-analytical sample processing in maintaining the metabolic integrity of plasma samples. Accordingly, we adhered stringently to optimal practices for sample storage, handling, and transportation before conducting the analysis.

However, there are still some limitations. Firstly, the identification of low-abundant metabolites remains challenging due to the complexity and wide dynamic range of analytes in plasma, which often can impede their identification through LC-MS analysis. Secondly, the study's cross-sectional design limits our ability to determine whether the observed metabolite changes are pathogenic or secondary to disease processes, underscoring the need for longitudinal studies. Thirdly, this study did not include cerebrospinal fluid (CSF) analysis, which could provide additional insights. Future research could focus on identifying metabolic biomarkers in CSF and broadening the scope to compare with groups such as mild cognitive impairment (MCI) and PD. Finally, the metabolites identified in our study need further external validation and

animal experiments validation to confirm causality, and through absolute quantitative assays utilizing target metabolic histology.

Conclusion

In this study, we identified a distinctive lipid profile in the plasma of individuals diagnosed with DLB. Notably, specific lipid subclasses, particularly sphingolipids (e.g., Cers and SPH) and phospholipid (e.g., PA, PE and PC) were markedly dysregulated in DLB patients. This finding implies a heightened susceptibility of cellular membranes to DLB-mediated pathological alterations. Furthermore, significant correlations were noted between these lipidomic signatures and both the UPDRS III as well as cognitive performance metrics. This correlation highlights the potential relevance of these lipidomic signatures in assessing the severity of DLB symptoms. In addition, the study identified two lipidomic panels that not only facilitate the identification of DLB subjects but also contribute to differentiating DLB from AD, which indicates that these lipidomic panels may serve as effective plasma biomarkers for the diagnosis of DLB or for distinguishing between different forms of dementia. Our future research will focus on elucidating the clinical relevance of these lipidomic signatures and exploring their potential for integration into diagnostic and therapeutic frameworks for DLB.

Abbreviations

DLB	Dementia with Lewy bodies
AD	Alzheimer's diseases
HCs	Healthy controls
MMSE	Mini-Mental State Examination
MoCA	Montreal cognitive assessment
CDT	Clock Drawing Test
CDR	Clinical Dementia Rating Scale
UPDRS	Unified Parkinson's Disease Rating Scale
REM	Rapid eye movement
RBD	REM sleep behavior disorder
MS	Mass spectrometry
AUC	Area Under the Curve
ROC	Receiver-operating characteristic
SPH	Sphingosine
CerG3GNAc1	Trihexosyl N-trihexosyl ceramide
CerG2GNAc1	Dihexosyl N-acetylhexosyl ceramide
Hex1Cer	Hexosylceramide
Hex3Cer	Trihexosylceramide
FA	Fatty acids
WE	Wax esters
LPC	Lysophosphatidylcholine
LPG	Lysophosphatidylglycerol
LPE	Lysophosphatidylethanolamine
LPI	Lysophosphatidylinositol
PA	Phosphatidic acid
PC	Phosphatidylcholine
PE	Phosphatidylethanolamine
SM	Sphingomyelin
TG	Triglyceride
Cers	Ceramides
CL	Cardiolipin
ChE	Cholesteryl ester

Supplementary Information

The online version contains supplementary material available at https://doi.org/10.1186/s13195-024-01585-7.

Supplementary Material 1: Supplementary Table S1. Putative identity of the significantly differentially expressed lipids between DLB patients and HCs. Abbreviations: DLB, dementia with Lewy bodies; HCs, healthy control. Supplementary Table S2. Putative identity of the significantly differentially expressed lipids between DLB patients and HCs (Analysis of covariance). Abbreviations: DLB, dementia with Lewy bodies; HCs, healthy control. Adjusted for age and gender. Supplementary Table S3. Putative identity of the significantly differentially expressed lipids between DLB and AD patients. Abbreviations: DLB, dementia with Lewy bodies; AD, Alzheimer's diseases. Supplementary Table S4. Putative identity of the significantly differentially expressed lipids between DLB and AD patients (Analysis of covariance). Abbreviations: DLB, dementia with Lewy bodies; AD, Alzheimer's diseases. Adjusted for age and gender

Acknowledgments

The authors are grateful to all of the participants in this study.

Authors' contributions

MQ and YT designed and conceptualized the study. HXS and YYY searched the literature. HXS, YTN and JW conducted the clinical investigation and collected the data. HXS and YYY analyzed the data. HXS and MQ wrote the manuscript draft. All authors revised the manuscript and approved it for submission.

Funding

This work was supported by grants from the National Key R&D Program of China (2020YFC2003100, 2020YFC2003103).

Data availability

No datasets were generated or analysed during the current study.

Declarations

Ethic approval and consent to participate

This study was approved by the Ethics Committee of Xuanwu Hospital, Capital Medical University (approval No. [2020]141), which complies with the Declaration of Helsinki. Written informed consent was obtained from the patient and their guardian.

Consent for publication

Not applicable.

Competing interests

The authors declare no competing interests.

Author details

[1]Departments of Neurology, Xuanwu Hospital, Capital Medical University, Beijing 100053, China. [2]Innovation Center for Neurological Disorders, Department of Neurology, Xuanwu Hospital, Capital Medical University, Beijing, China. [3]Department of Neurology & Innovation Center for Neurological Disorders, Xuanwu Hospital, Capital Medical University, Beijing 100053, China. [4]Departments of Chinese Medicine, Xuanwu Hospital, Capital Medical University, Beijing, China. [5]School of Life Sciences, Beijing University of Chinese Medicine, Beijing, China.

Received: 29 April 2024 Accepted: 29 September 2024
Published online: 15 October 2024

References

1. Global status report. on the public health response to dementia. Geneva: World Health Organization; 2021.
2. McKeith I, Mintzer J, Aarsland D, Burn D, Chiu H, Cohen-Mansfield J, et al. Dementia with Lewy bodies. LANCET NEUROL. 2004;3:19–28.

3. McKeith IG, Boeve BF, Dickson DW, Halliday G, Taylor JP, Weintraub D, et al. Diagnosis and management of dementia with Lewy bodies: Fourth consensus report of the DLB Consortium. NEUROLOGY. 2017;89:88–100.
4. Vann JS, JT O'Brien. The prevalence and incidence of dementia with Lewy bodies: a systematic review of population and clinical studies. PSYCHOL MED. 2014;44:673–83.
5. Ferman TJ, Aoki N, Crook JE, Murray ME, Radford NRG, Gerpen JA, et al. The limbic and neocortical contribution of α-synuclein, tau, and amyloid β to disease duration in dementia with Lewy bodies. Alzheimer's Dement. 2018;14:330–9.
6. McKeith IG, Dickson DW, Lowe J, Emre M, O'Brien JT, Feldman H, et al. Diagnosis and management of dementia with Lewy bodies: Third report of the DLB consortium. NEUROLOGY. 2005;65:1863–72.
7. Kemp J, Philippi N, Phillipps C, Demuynck C, Albasser T, Martin-Hunyadi C, et al. Cognitive profile in prodromal dementia with Lewy bodies. Alzheimers Res Ther. 2017;9:19.
8. Mapstone M, Cheema AK, Fiandaca MS, Zhong X, Mhyre TR, MacArthur LH, et al. Plasma phospholipids identify antecedent memory impairment in older adults. NAT MED. 2014;20:415–8.
9. Whiley L, Sen A, Heaton J, Proitsi P, García-Gómez D, Leung R, et al. Evidence of altered phosphatidylcholine metabolism in Alzheimer's disease. NEUROBIOL AGING. 2014;35:271–8.
10. Wang J, Wei R, Xie G, Arnold M, Kueider-Paisley A, Louie G, et al. Peripheral serum metabolomic profiles inform central cognitive impairment. SCI REP-UK. 2020;10:14059.
11. Huo Z, Yu L, Yang J, Zhu Y, Bennett DA, Zhao J. Brain and blood metabolome for Alzheimer's dementia: findings from a targeted metabolomics analysis. NEUROBIOL AGING. 2020;86:123–33.
12. Hunsberger HC, Greenwood BP, Tolstikov V, Narain NR, Kiebish MA, Denny CA. Divergence in the metabolome between natural aging and Alzheimer's disease. SCI REP-UK. 2020;10:19863.
13. Niedzwiecki MM, Walker DI, Howell JC, Watts KD, Jones DP, Miller GW, et al. High-resolution metabolomic profiling of Alzheimer's disease in plasma. ANN CLIN TRANSL NEUR. 2020;7:36–45.
14. Orešič M, Hyötyläinen T, Herukka S, Sysi-Aho M, Mattila I, Seppänan-Laakso T, et al. Metabolome in progression to Alzheimer's disease. TRANSL PSYCHIAT. 2011;1:e57.
15. Cuperlovic-Culf M, Badhwar A. Recent advances from metabolomics and lipidomics application in alzheimer's disease inspiring drug discovery. EXPERT OPIN DRUG DIS. 2020;15:319–31.
16. Fu Y, He Y, Phan K, Bhatia S, Pickford R, Wu P, et al. Increased unsaturated lipids underlie lipid peroxidation in synucleinopathy brain. ACTA NEUROPATHOL COM. 2022;10:165.
17. Fanning S, Selkoe D, Dettmer U. Vesicle trafficking and lipid metabolism in synucleinopathy. ACTA NEUROPATHOL. 2021;141:491–510.
18. Olsson BD, Lautner RM, Andreasson UP, Öhrfelt AP, Portelius EP, Bjerke MP, et al. CSF and blood biomarkers for the diagnosis of Alzheimer's disease: a systematic review and meta-analysis. LANCET NEUROL. 2016;15:673–84.
19. Janelidze S, Mattsson N, Palmqvist S, Smith R, Beach TG, Serrano GE, et al. Plasma P-tau181 in Alzheimer's disease: relationship to other biomarkers, differential diagnosis, neuropathology and longitudinal progression to Alzheimer's dementia. NAT MED. 2020;26:379–86.
20. McKhann GM, Knopman DS, Chertkow H, Hyman BT, Jack CR, Kawas CH, et al. The diagnosis of dementia due to Alzheimer's disease: Recommendations from the National Institute on Aging-Alzheimer's Association workgroups on diagnostic guidelines for Alzheimer's disease. Alzheimer's Dement. 2011;7:263–9.
21. Jack CR, Bennett DA, Blennow K, Carrillo MC, Dunn B, Haeberlein SB, et al. NIA-AA Research Framework: Toward a biological definition of Alzheimer's disease. Alzheimer's Dement. 2018;14:535–62.
22. Mueller CD, Ballard CP, Corbett AP, Aarsland DP. The prognosis of dementia with Lewy bodies. LANCET NEUROL. 2017;16:390–8.
23. González-Domínguez R, González-Domínguez Á, Sayago A. Á Fernández-Recamales. Recommendations and Best Practices for Standardizing the Pre-Analytical Processing of Blood and Urine Samples in Metabolomics. METABOLITES. 2020;10:229.
24. Zhang L, Bi S, Liang Y, Huang L, Li Y, Huang M, et al. Integrated Metabolomic and Lipidomic Analysis in the Placenta of Preeclampsia. FRONT PHYSIOL. 2022;13:807583.
25. Wang H, Zhou Q, Wan L, Guo M, Chen C, Xue J, et al. Lipidomic analysis of meibomian glands from type-1 diabetes mouse model and preliminary studies of potential mechanism. EXP EYE RES. 2021;210:108710.
26. Holčapek M, Liebisch G, Ekroos K. Lipidomic Anal ANAL CHEM. 2018;90:4249–57.
27. Taguchi R, Ishikawa M. Precise and global identification of phospholipid molecular species by an Orbitrap mass spectrometer and automated search engine Lipid Search. J CHROMATOGR A. 2010;1217:4229–39.
28. Bartke N, Hannun YA. Bioactive sphingolipids: metabolism and function. J LIPID RES. 2009;50:S91–6.
29. Hussain G, Wang J, Rasul A, Anwar H, Imran A, Qasim M, et al. Role of cholesterol and sphingolipids in brain development and neurological diseases. LIPIDS HEALTH DIS. 2019;18:26.
30. Mielke MM, Lyketsos CG. Alterations of the Sphingolipid Pathway in Alzheimer's Disease: New Biomarkers and Treatment Targets? NEUROMOL MED. 2010;12:331–40.
31. JW PETTEGREW, K PANCHALINGAM RLHAMILTON, RJ MCCLURE. Brain membrane phospholipid alterations in Alzheimer's disease. NEUROCHEM RES. 2001;26:771–82.
32. He X, Huang Y, Li B, Gong C, Schuchman EH. Deregulation of sphingolipid metabolism in Alzheimer's disease. NEUROBIOL AGING. 2010;31:398–408.
33. Yuyama K, Mitsutake S, Igarashi Y. Pathological roles of ceramide and its metabolites in metabolic syndrome and Alzheimer's disease. Biochim et Biophys Acta (BBA) - Mol Cell Biology Lipids. 2014;1841:793–8.
34. Nie Y, Chu C, Qin Q, Shen H, Wen L, Tang Y, et al. Lipid metabolism and oxidative stress in patients with Alzheimer's disease and amnestic mild cognitive impairment. BRAIN PATHOL. 2024;34:e13202.
35. Mielke MM, Bandaru VVR, Haughey NJ, Rabins PV, Lyketsos CG, Carlson MC. Serum sphingomyelins and ceramides are early predictors of memory impairment. NEUROBIOL AGING. 2010;31:17–24.
36. Tringali C, Giussani P. Ceramide and Sphingosine-1-Phosphate in Neurodegenerative Disorders and Their Potential Involvement in Therapy. Int J Mol Sci. 2022;23:7806.
37. Simuni T, Chahine LM, Poston K, Brumm M, Buracchio T, Campbell M, et al. A biological definition of neuronal alpha-synuclein disease: towards an integrated staging system for research. LANCET NEUROL. 2024;23:178–90.
38. Mielke MM, Maetzler W, Haughey NJ, Bandaru VV, Savica R, Deuschle C, et al. Plasma ceramide and glucosylceramide metabolism is altered in sporadic Parkinson's disease and associated with cognitive impairment: a pilot study. PLoS ONE. 2013;8:e73094.
39. Schwedhelm E, Englisch C, Niemann L, Lezius S, von Lucadou M, Marmann K, et al. Sphingosine-1-Phosphate, Motor Severity, and Progression in Parkinson's Disease (MARK-PD). Mov DISORD. 2021;36:2178–82.
40. Pépin É, Jalinier T, Lemieux GL, Massicotte G, Cyr M. Sphingosine-1-Phosphate Receptors Modulators Decrease Signs of Neuroinflammation and Prevent Parkinson's Disease Symptoms in the 1-Methyl-4-Phenyl-1,2,3,6-Tetrahydropyridine Mouse Model. FRONT PHARMACOL. 2020;11:77.
41. Vidal-Martinez G, Najera K, Miranda JD, Gil-Tommee C, Yang B, Vargas-Medrano J, et al. FTY720 Improves Behavior, Increases Brain Derived Neurotrophic Factor Levels and Reduces α-Synuclein Pathology in Parkinsonian GM2 +/– Mice. Neuroscience. 2019;411:1–10.
42. Stunff HL, Milstien S, Spiegel S. Generation and metabolism of bioactive sphingosine-1-phosphate. J CELL BIOCHEM. 2004;92:882–99.
43. Katsel P, Li C. Gene Expression Alterations in the Sphingolipid Metabolism Pathways during Progression of Dementia and Alzheimer's Disease: A Shift Toward Ceramide Accumulation at the Earliest Recognizable Stages of Alzheimer's Disease? NEUROCHEM RES. 2007;32:845–56.
44. He X, Huang Y, Li B, Gong C, Schuchman EH. Deregulation of sphingolipid metabolism in Alzheimer's disease. NEUROBIOL AGING. 2010;31:398–408.
45. Huang Y, Tanimukai H, Liu F, Iqbal K, Iqbal IG, Gong CX. Elevation of the level and activity of acid ceramidase in Alzheimer's disease brain. EUR J NEUROSCI. 2004;20:3489–97.
46. Czubowicz K, Jęśko H, Wencel P, Lukiw WJ, Strosznajder RP. The Role of Ceramide and Sphingosine-1-Phosphate in Alzheimer's Disease and Other Neurodegenerative Disorders. MOL NEUROBIOL. 2019;56:5436–55.
47. Abbott SK, Li H, Muñoz SS, Knoch B, Batterham M, Murphy KE, et al. Altered ceramide acyl chain length and ceramide synthase gene expression in Parkinson's disease. Mov DISORD. 2014;29:518–26.
48. Lin G, Lee P, Chen K, Mao D, Tan KL, Zuo Z, et al. Phospholipase PLA2G6, a Parkinsonism-Associated Gene, Affects Vps26 and Vps35, Retromer Function, and Ceramide Levels, Similar to α-Synuclein Gain. CELL METAB. 2018;28:605–18.
49. Sidransky E, Nalls MA, Aasly JO, Aharon-Peretz J, Annesi G, Barbosa ER, et al. Multicenter Analysis of Glucocerebrosidase Mutations in Parkinson's Disease. NEW ENGL J MED. 2009;361:1651–61.

50. Kumar KR, Ramirez A, Göbel A, Kresojević N, Svetel M, Lohmann K, et al. Glucocerebrosidase mutations in a Serbian Parkinson's disease population. EUR J NEUROL. 2013;20:402–5.
51. Murphy KE, Gysbers AM, Abbott SK, Tayebi N, Kim WS, Sidransky E, et al. Reduced glucocerebrosidase is associated with increased α-synuclein in sporadic Parkinson's disease. Brain. 2014;137:834–48.
52. Gegg ME, Burke D, Heales SJ, Cooper JM, Hardy J, Wood NW, et al. Glucocerebrosidase deficiency in substantia nigra of parkinson disease brains. ANN NEUROL. 2012;72:455–63.
53. Pchelina S, Emelyanov A, Baydakova G, Andoskin P, Senkevich K, Nikolaev M, et al. Oligomeric α-synuclein and glucocerebrosidase activity levels in GBA-associated Parkinson's disease. NEUROSCI LETT. 2017;636:70–6.
54. Wright MM, McMaster CR. PC and PE synthesis: mixed micellar analysis of the cholinephosphotransferase and ethanolaminephosphotransferase activities of human choline/ethanolamine phosphotransferase 1 (CEPT1). Lipids. 2002;37:663–72.
55. Cheng D, Jenner AM, Shui G, Cheong WF, Mitchell TW, Nealon JR, et al. Lipid pathway alterations in Parkinson's disease primary visual cortex. PLoS ONE. 2011;6:e17299.
56. Wood PL, Tippireddy S, Feriante J, Woltjer RL. Augmented frontal cortex diacylglycerol levels in Parkinson's disease and Lewy Body Disease. PLoS ONE. 2018;13:e0191815.
57. Hattingen E, Magerkurth J, Pilatus U, Mozer A, Seifried C, Steinmetz H, et al. Phosphorus and proton magnetic resonance spectroscopy demonstrates mitochondrial dysfunction in early and advanced Parkinson's disease. Brain. 2009;132:3285–97.
58. Stoessel D, Schulte C, Teixeira DSM, Scheller D, Rebollo-Mesa I, Deuschle C, et al. Promising Metabolite Profiles in the Plasma and CSF of Early Clinical Parkinson's Disease. FRONT AGING NEUROSCI. 2018;10:51.
59. Galvagnion C, Buell AK, Meisl G, Michaels TCT, Vendruscolo M, Knowles TPJ, et al. Lipid vesicles trigger α-synuclein aggregation by stimulating primary nucleation. NAT CHEM BIOL. 2015;11:229–34.
60. Grey M, Dunning CJ, Gaspar R, Grey C, Brundin P, Sparr E, et al. Acceleration of α-Synuclein Aggregation by Exosomes. J BIOL CHEM. 2015;290:2969–82.
61. De Franceschi G, Frare E, Pivato M, Relini A, Penco A, Greggio E, et al. Structural and Morphological Characterization of Aggregated Species of α-Synuclein Induced by Docosahexaenoic Acid. J BIOL CHEM. 2011;286:22262–74.
62. Galvagnion C, Brown JWP, Ouberai MM, Flagmeier P, Vendruscolo M, Buell AK, et al. Chemical properties of lipids strongly affect the kinetics of the membrane-induced aggregation of α-synuclein. Proc Natl Acad Sci. 2016;113:7065–70.
63. Mizuno S, Sasai H, Kume A, Takahashi D, Satoh M, Kado S, et al. Dioleoylphosphatidic acid selectively binds to α-synuclein and strongly induces its aggregation. FEBS LETT. 2017;591:784–91.

Publisher's Note